EPJ Web of Conferences **20**, 01007 (2012)
DOI: 10.1051/epjconf/20122001007

Quark models for mesons

Jialun Ping[1,a], Chengrong Deng[2], Hongxia Huang[1], Fangfang Dong[1], Fan Wang[3]

[1]Department of Physics, Nanjing Normal University, Nanjing 210097, P.R. China
[2]School of Mathematics and Physics, Chongqing Jiaotong University, Chongqing 400074, P.R. China
[3]Department of Physics, Nanjing University, Nanjing 210093, P.R. China

Abstract. With the advance of experiment, many high excited states of meson are identified. It is found that many of them are difficult to fit into conventional $q\bar{q}$ meson spectra. Various explanations are proposed. One of them is the four-quark states or molecules of two mesons. In the framework of quark model, by taking into account of multi-body interaction, four-quark states are studied. The results show that the scalar mesons: $f_0(600)$,$f_0(980)$ and $Y(2175)$ can be well described by four-quark states. Furthermore, unquenched quark model, which incorporates the four-quark components in the conventional $q\bar{q}$ states, is constructed for mesons. By readjusting the model parameters, the model can give a good description of mesons. The model is also used to study the newly discovered XYZ particles.

1 Introduction

Hadrons (meson and baryon) are the strong interacting systems, which are the main source we get the information of quantum chromodynamics (QCD), the fundamental theory of strong interaction. Because of the complexity and the non-perturbative property of QCD in low-energy region, To get a reliable results for hadrons is still a challenge task for QCD. Although lattice QCD, QCD sum-rule, Dyson-schwinger approach and other non-perturbative method make some impressive progresses recently, the QCD-inspired quark model is still a powerful and common used method to study the properties of hadrons.

In quark models, the naive picture of meson ($q\bar{q}$) and baryon (qqq) achieved a tremendous success on the properties of hadrons due to the unique color structure of hadrons. However it also limits us to obtain the more information on color properties of QCD. Multiquark system is indispensable to explore the various color structure of QCD [1]. In fact, there are many high Fock components in a meson state in addition to $q\bar{q}$,

$$|M\rangle = |q\bar{q}\rangle + |q\bar{q}q\bar{q}\rangle + |q\bar{q}g\rangle + |q^3\bar{q}^3\rangle + \cdots \tag{1}$$

In naive quark model, the effects of high Fock states are renormalized into the parameters. In most case, it is a good approximation, especially for ground state hadrons with heavy quarks. Recently, BaBar, Belle and other collaborations discovered some new charmonium-like states ("XYZ" states) above the open charm threshold, which is difficult to fit into the conventional pictures of $c\bar{c}$ mesons [2]. A lot of explanations are proposed for "XYZ" states, tetraquark states, molecular states, hybrid, charmonium, etc. [2].

To unify the description of mesons, the construction of unquenched quark model is needed. In the unquenched approach, the high Fock components are taken into account. The present work is trying to study the charmonium spectrum by including the four-quark component in addition to $q\bar{q}$ in the calculation.

[a] e-mail: jlping@njnu.edu.cn

The structure of the paper is as follows, Sect. 2 gives a brief introduction of the conventional quark model, the chiral quark model. A string-like quark model is introduce in Sect. 3 and apply to four-quark system. The unquenched quark model for $c\bar{c}$ is given in Sect.4. Finally a summary is given in the last section.

2 Constituent Quark Models

The important properties of QCD in the low-energy region are color confinement and the spontaneous breaking of chiral symmetry. The spontaneous breaking of chiral symmetry leads to that the quarks obtain their constituent masses and interact with each other through the exchange of Goldstone bosons [3]. The color confinement is imitated by introducing color confinement potential and the perturbative part of QCD is retained by effective one gluon exchange in quark model. Generally the chiral partner σ-meson is invoked to account for the intermediate-range attraction of nucleon-nucleon interaction in the chiral quark model and the chiral quark gives a good description of meson spectrum [4]. However, there are some controversies on the use of σ-meson and it is argued recently that the σ-meson exchange used in the chiral quark model can be replaced by the quark delocalization and color screening mechanism [5]. In the following we show that the quark model without σ-meson exchange can also describe the meson spectrum well. The model Hamiltonian of the $q\bar{q}$ system ($n = 2$) is

$$H = \sum_{i=1}^{n}\left(m_i + \frac{\mathbf{p}_i^2}{2m_i}\right) - T_{CM} + \sum_{i>j}^{n}(V_{ij}^C + V_{ij}^G + V_{ij}^\chi), \quad \chi = \pi, K, \eta \tag{2}$$

$$V_{ij}^\pi = \frac{g_{ch}^2}{4\pi}\frac{m_\pi^2}{12m_im_j}\frac{\Lambda_\pi^2}{\Lambda_\pi^2 - m_\pi^2}m_\pi\sigma_i\cdot\sigma_j\left[Y(m_\pi\, r_{ij}) - \frac{\Lambda_\pi^3}{m_\pi^3}Y(\Lambda_\pi r_{ij})\right]\sum_{a=1}^{3}F_i^a\cdot F_j^a \tag{3}$$

$$V_{ij}^K = \frac{g_{ch}^2}{4\pi}\frac{m_K^2}{12m_im_j}\frac{\Lambda_K^2}{\Lambda_K^2 - m_\pi^2}m_K\sigma_i\cdot\sigma_j\left[Y(m_K\, r_{ij}) - \frac{\Lambda_K^3}{m_K^3}Y(\Lambda_K r_{ij})\right]\sum_{a=4}^{7}F_i^a\cdot F_j^a \tag{4}$$

$$V_{ij}^\eta = \frac{g_{ch}^2}{4\pi}\frac{m_\eta^2}{12m_im_j}\frac{\Lambda_\eta^2}{\Lambda_\eta^2 - m_\eta^2}m_\eta\sigma_i\cdot\sigma_j\left[Y(m_\eta\, r_{ij}) - \frac{\Lambda_\eta^3}{m_\eta^3}Y(\Lambda_\eta r_{ij})\right]\left[\cos\theta_P(F_i^8\cdot F_j^8) - \sin\theta_P\right], \tag{5}$$

$$V_{ij}^G = \frac{1}{4}\alpha_s\lambda_i^c\cdot\lambda_j^c\left[\frac{1}{r_{ij}} - \frac{\pi}{2}\delta(\mathbf{r}_{ij})\left(\frac{1}{m_i^2} + \frac{1}{m_j^2} + \frac{4}{3m_im_j}\sigma_i\cdot\sigma_j\right)\right], \tag{6}$$

$$V_{ij}^C = k(r_{ij}^2 - \Delta). \tag{7}$$

where T_{CM} is the center-of-mass kinetic energy, $Y(x)$ is the standard Yukawa function and all symbols have their usual meaning. The delta function in the one-gluon exchange potential should be regularized because of the finite size of the constituent quark [6], the regularization is flavor dependent [4,7],

$$\delta(\mathbf{r}_{ij}) = \frac{1}{4\pi}\frac{1}{r_{ij}r_0^2(\mu)}e^{-r_{ij}/r_0(\mu)}, \tag{8}$$

where μ is the reduced mass of the $q\bar{q}$ system and $r_0(\mu) = \hat{r}_0/\mu$ and the $\hat{r}_0$ is a model parameter.

The model parameters are fixed as follows: the u, d-quark masses are taken as the same and are assumed to be exactly $\frac{1}{3}$ of the nucleon mass, namely $m_u = m_d = 313$ MeV, the masses of π, K, η take the experimental values, the Λ_π, Λ_K, Λ_η, θ_p, Λ_0 and μ_0 are taken the same values as in Ref.[4], namely $\Lambda_\pi = 4.2$ fm^{-1}, $\Lambda_K = \Lambda_\eta = 5.2$ fm^{-1}, θ_p=-15°, $\Lambda_0 = 36.98$ MeV and $\mu_0 = 0.113$ fm. The chiral coupling constant g_{ch} is determined from the πNN coupling constant through

$$\frac{g_{ch}^2}{4\pi} = \left(\frac{3}{5}\right)^2\frac{g_{\pi NN}^2}{4\pi}\frac{m_{u,d}^2}{m_N^2} \tag{9}$$

and flavor $SU(3)$ symmetry is assumed, where $\frac{g_{ch}^2}{4\pi}$=0.54. The rest parameters m_s, k, Δ, α_0 and $\hat{r}_0$ are determined by fitting ground state meson spectra. An effective scale-dependent strong coupling constant [4] is given by

$$\alpha_s(\mu) = \frac{\alpha_0}{\ln\left[\frac{\mu^2+\mu_0^2}{\Lambda_0^2}\right]}. \tag{10}$$

The meson spectra are obtained by solving the following Schrödinger equation

$$\left[-\frac{\hbar^2}{2\mu}\nabla^2 + V(\mathbf{r}) - E\right]\psi_{lm}(\mathbf{r})\psi_{csf} = 0 \tag{11}$$

where ψ_{lm} is the relative orbital motion wave functions, ψ_{csf} is the color-spin-flavor wave function. $\psi_{lm}(\mathbf{r})$ can be expanded by means of Gaussian functions with different size [8]

$$\phi_{lm}(\mathbf{r}) = \sum_{n=1}^{n_{max}} c_n N_{nl} r^l e^{-\nu_n r^2} Y_{lm}(\hat{\mathbf{r}}). \tag{12}$$

Gaussian size parameters are taken as geometric progression

$$\nu_n = \frac{1}{r_n^2},\ r_n = r_1 a^{n-1},\ a = \left(\frac{r_{n_{max}}}{r_1}\right)^{\frac{1}{n_{max}-1}}. \tag{13}$$

With $r_1 = 0.1$ fm, $r_{n_{max}} = 2.0$ fm and $n_{max} = 7$, we can obtain converged results. The model parameters and part of the obtained meson masses are shown in the Table 1 and 2, respectively. The more detailed results can be seen in Ref.[9].

Table 1. The model parameters.

m_s (MeV)	m_c (MeV)	k (MeV fm^{-2})	$\hat{r}_0$ (MeV fm)	Δ (fm^2)	α_0
520	1700	213.3	30.85	0.5	4.25

Table 2. Meson spectra (MeV).

Meson:	π	K	ρ	K^*	ω	ϕ
Theo. ($L=0$)	139	502	761	897	735	1023
Exp. ($L=0$)	139	496	770	898	780	1020
Theo. ($L=1$)	1054	1204	1102	1226	1098	1342
Meson:	D^0	D^*	D_s	D_s^*	η_c	J/ψ
Theo. ($L=0$)	1928	2001	2014	2112	2992	3144
Exp. ($L=0$)	1865	2007	1968	2112	2980	3097
Theo. ($L=1$)	2304	2310	2401	2405	3419	3420

From Table 2, one can see that the calculated meson masses are consistent with experimental values. The masses of mesons with orbital angular momentum $L = 1$ are also given in Table 2. As in other work, the low-lying scalar mesons, $f_0(600)$, $f_0(980), \cdots$ and most newly observed states $Y(2175)$, $X(3872)$, $\cdots$, can not be described well in the model. A possible reason is that those states are tetraquark states, which we present in the following section.

3 The String model for tetraquark states

In multiquark system, the interaction among quarks is genuinely a multi-body interaction. The recent calculation of lattice QCD on the two-, three-, four- and five-quark systems show that the interactions

among quarks can be approximated by the following formula [10],

$$V_{q\bar{q}} = -A_{q\bar{q}}\frac{1}{|\mathbf{r}_q - \mathbf{r}_{\bar{q}}|} + \sigma_{q\bar{q}}|\mathbf{r}_q - \mathbf{r}_{\bar{q}}| + C_{q\bar{q}}, \tag{14}$$

$$V_{q^3} = -A_{q^3}\sum_{i>j}\frac{1}{|\mathbf{r}_i - \mathbf{r}_j|} + \sigma_{q^3}L_{\min} + C_{q^3}, \tag{15}$$

$$V_{q^2\bar{q}^2} = -A_{q^2\bar{q}^2}\sum_{i>j}\frac{1}{|\mathbf{r}_i - \mathbf{r}_j|} + \sigma_{q^2\bar{q}^2}L_{\min} + C_{q^2\bar{q}^2}, \tag{16}$$

$$V_{q^4\bar{q}} = -A_{q^4\bar{q}}\sum_{i>j}\frac{1}{|\mathbf{r}_i - \mathbf{r}_j|} + \sigma_{q^4\bar{q}}L_{\min} + C_{q^4\bar{q}}, \tag{17}$$

$$L_{\min} = \sum_i L_i \tag{18}$$

where L_i is the length of the i-th string which connecting quarks and/or junctions. The universality of the "confinement" is shown by

$$\sigma_{q\bar{q}} = \sigma_{q^3} = \sigma_{q^2\bar{q}^2} = \sigma_{q^4\bar{q}} \tag{19}$$

The Casimir scaling in baryon and meson is justified by $A_{q\bar{q}} = 2A_{q^3}$.

Based on these calculations, a string (flux-tube) model is constructed [1]. For four-quark system, diquark-anti-diquark picture is often used because of the attractive property of diquark [11–14]. Here the picture is used to study the tetraquark state in the flux-tube model. The configuration is shown in Fig.1, where a quark (antiquark) is represented by a solid (hollow) dot, $\mathbf{r}_i$ is (anti)quark's position, $\mathbf{y}_i$ is the junction where three strings (flux tubes) meet. A thin line connecting a quark and a junction represents a fundamental representation, *i.e.* color triplet, and a thick line connecting two junctions is for a color sextet or other representations, namely a compound string. The different types of string may have different stiffness [15, 16]. The overall color singlet is satisfied by the coupling $[[qq]_{\mathbf{3}}[\bar{q}\bar{q}]_{\mathbf{3}}]_{\mathbf{1}}$ and $[[qq]_{\mathbf{6}}[\bar{q}\bar{q}]_{\bar{\mathbf{6}}}]_{\mathbf{1}}$, subscripts represent the dimensions of color representations.

In the flux-tube model, the confinement potential of the tetraquark state takes the following form (To simplify the calculation, the length of the string is replaced by the square of the length),

$$V^C = k\left[(\mathbf{r}_1 - \mathbf{y}_1)^2 + (\mathbf{r}_2 - \mathbf{y}_1)^2 + (\mathbf{r}_3 - \mathbf{y}_2)^2(\mathbf{r}_4 - \mathbf{y}_2)^2 + \kappa_d(\mathbf{y}_1 - \mathbf{y}_2)^2\right], \tag{20}$$

where k is the stiffness of the string with the fundamental representation **3** and $k\kappa_d$ is the compound string stiffness, which can be obtained by [16]

$$\kappa_{\mathbf{d}} = \frac{C_{\mathbf{d}}}{C_{\mathbf{3}}}, \tag{21}$$

where $C_{\mathbf{d}}$ is the eigenvalue of the Casimir operator associated with the $SU(3)$ color representation **d** of the string, $C_{\mathbf{3}} = \frac{4}{3}$, $C_{\mathbf{6}} = \frac{10}{3}$ and $C_{\mathbf{8}} = 3$.

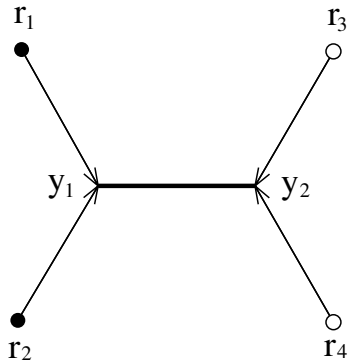

Fig. 1. Diquark-antidiquark state.

For the given $\mathbf{r}_i$'s, the $\mathbf{y}_i$'s are fixed by minimizing the energy of the system. With fixed $\mathbf{y}_i$'s and in the center of mass coordinate, the potential reduces to

$$V^C = \frac{k}{m}\left(\mathbf{Q}_1^2 + \mathbf{Q}_2^2 + \frac{\kappa_d}{1+\kappa_d}\mathbf{Q}_3^2\right) \tag{22}$$

where the canonical coordinates take the following form

$$\begin{aligned}
\mathbf{Q}_1 &= \sqrt{\frac{m}{2}}(\mathbf{r}_1 - \mathbf{r}_2), \\
\mathbf{Q}_2 &= \sqrt{\frac{m}{2}}(\mathbf{r}_3 - \mathbf{r}_4), \\
\mathbf{Q}_3 &= \sqrt{\frac{m}{4}}(\mathbf{r}_1 + \mathbf{r}_2 - \mathbf{r}_3 - \mathbf{r}_4), \\
\mathbf{Q}_4 &= \sqrt{\frac{m}{4}}(\mathbf{r}_1 + \mathbf{r}_2 + \mathbf{r}_3 + \mathbf{r}_4).
\end{aligned} \tag{23}$$

if all quarks have the same mass. Taking into account of the potential energy shift (see Eq.(7) above), the confinement potential V^C used in the present calculation has the following form

$$V^C = k\left[\left(\frac{(\mathbf{r}_1 - \mathbf{r}_2)^2}{2} - \Delta\right) + \left(\frac{(\mathbf{r}_3 - \mathbf{r}_4)^2}{2} - \Delta\right) + \frac{\kappa_d}{1+\kappa_d}\left(\left(\frac{\mathbf{r}_1 + \mathbf{r}_2}{2} - \frac{\mathbf{r}_3 + \mathbf{r}_4}{2}\right)^2 - \Delta\right)\right] \tag{24}$$

Clearly our confinement potential is a multi-body interaction. The Hamiltonian for the four-quark system has the same as Eq.(2) with $n = 4$ and replacing the confinement potential by Eq.(24).

The wave function of the four-quark system is

$$\Phi_{IJ_TM_T} = \left[\left[\left[\phi^G_{l_1m_1}(\mathbf{r})\Psi_{s_1m_{s_1}}\right]_{J_1M_1}\left[\psi^G_{l_2m_2}(\mathbf{R})\Psi_{s_2m_{s_2}}\right]_{J_2M_2}\right]_{J_{12}M_{12}}\chi^G_{LM}(\mathbf{X})\right]_{J_TM_T}\left[\Psi_{c_1}\Psi_{c_2}\right]_c\left[\Psi_{I_1}\Psi_{I_2}\right]_I, \tag{25}$$

where I_i, s_i and c_i , $i = 1, 2$ represent isospin, spin and color of diquark and anti-diquark, respectively. The Jacobi coordinates are defined as

$$\mathbf{r} = \mathbf{r}_1 - \mathbf{r}_2, \quad \mathbf{R} = \mathbf{r}_3 - \mathbf{r}_4, \quad \mathbf{X} = \frac{\mathbf{r}_1 + \mathbf{r}_2}{2} - \frac{\mathbf{r}_3 + \mathbf{r}_4}{2}. \tag{26}$$

The four-quark state is an overall color singlet with well defined parity $P = (-1)^{l_1+l_2+L}$, isospin I and total angular momentum J_T.

The energy of the tetraquark states can be obtained by solving the four-body Schrödinger equation

$$(H - E)\Phi_{IJ_TM_T} = 0. \tag{27}$$

To obtain a reliable solution of few-body problem, a high precision method is indispensable. The Gaussian Expansion Method (GEM) [8], which has been proven to be powerful in nuclear and hadron physics, is employed here. In GEM, three relative motion wave functions are written as,

$$\phi^G_{l_1m_1}(\mathbf{r}) = \sum_{n_1=1}^{n_{1max}} c_{n_1} N_{n_1l_1} r^{l_1} e^{-\nu_{n_1}r^2} Y_{l_1m_1}(\hat{\mathbf{r}}) \tag{28}$$

$$\psi^G_{l_2m_2}(\mathbf{R}) = \sum_{n_2=1}^{n_{2max}} c_{n_2} N_{n_2l_2} R^{l_2} e^{-\nu_{n_2}R^2} Y_{l_2m_2}(\hat{\mathbf{R}}) \tag{29}$$

$$\chi^G_{LM}(\mathbf{X}) = \sum_{n_3=1}^{n_{3max}} c_{n_3} N_{LM} X^L e^{-\nu_{n_3} X^2} Y_{LM}(\hat{\mathbf{X}}) \tag{30}$$

The choice of Gaussian size is the same as that of mesons (see Eq.(13). In GEM the calculated results are converged with n_{1max}=10, n_{2max} = 10 and n_{3max} = 10. Minimum and maximum ranges of the bases are 0.1 fm and 3.0 fm for coordinates **r**, **R** and **X**, respectively.

The model is applied to study the tetraquark states: $n\bar{n}n\bar{n}$, $n = u, d$, $s\bar{s}s\bar{s}$, etc. Part of the results are shown in Table 3. In obtaining the results, all the possible channels are included. So the model space is generally constructed by several thousands basis functions, for example, $Y(2175)$, $I^G J^{PC} = 0^+1^{--}$, the number of basis functions is 2000.

Table 3. Energies for some tetraquark states (MeV). $n = u, d$.

States	$nn\bar{n}\bar{n}$	$nn\bar{n}\bar{n}$	$ns\bar{n}\bar{s}$	$ns\bar{n}\bar{s}$	$ss\bar{s}\bar{s}$	$ss\bar{s}\bar{s}$
$I^G J^{PC}$	0^+0^{++}	0^+0^{++}	1^-0^{++}	1^-1^{--}	0^+0^{++}	0^+1^{--}
Energy	587	1019	1306	1715	1925	2176
Candidate	$f_0(600)$	$f_0(980)$	$a_0(1450)$	$X(1576)$	$f_0(2020)$	$Y(2175)$
States	$cn\bar{c}\bar{n}$	$cn\bar{c}\bar{n}$	$cn\bar{c}\bar{n}$	$cn\bar{c}\bar{n}$	$cs\bar{c}\bar{s}$	$cs\bar{c}\bar{s}$
$I^G J^{PC}$	0^+1^{+-}	0^+0^{-+}	0^+0^{++}	0^+1^{--}	0^+0^{++}	0^+1^{--}
Energy	3776	4020	3644	3978	4038	4292
Candidate		$X(3872)$		$Y(4008)$		$Y(4260)$

From the Table 3, some interesting results are worth to mention. For non-strange tetraquark, the masses of ground state and the first radial excited state with quantum numbers $I^G J^{PC} = 0^+0^{++}$ are 587 MeV and 1019 MeV, which are very close to the experimental values of $f_0(600)$ and $f_0(980)$. So the scalar meson $f_0(600)$ and $f_0(980)$ can be identified as tetraquark states in the present calculation, other than the $q\bar{q}$ P-wave exited states (see Table 2). The same conclusion is also obtained in the study of the lowest-lying scalar mesons by the QCD sum rule [17]. Another interesting state is $Y(2175)$, which is observed by Babar Collaboration near the threshold in the process $e^+e^- \to \phi f_0(980)$ via initial-state radiation [18] and is confirmed by BES collaboration in the process $J/\psi \to \eta\phi f_0(980)$ [19]. The Breit-Wigner mass is $M = 2.175 \pm 0.010 \pm 0.015$GeV, and width is narrow $\Gamma = 0.058 \pm 0.016 \pm 0.020$GeV. The quantum numbers are claimed as $I^G J^{PC} = 0^+1^{--}$. Various theoretical interpretations have been proposed to explain this resonance, strangeonium hybrid [20]. tetraquark state $ss\bar{s}\bar{s}$ [21], S-wave threshold effects [22], ϕKK system [23], etc. In our calculation, A tetraquark state with diquark-anti-diquark structure can describe $Y(2175)$ very well. (For comparison, the state in the naive quark model and chiral quark model has much higher mass, 2422 MeV in the naive quark model and 2387 MeV in the chiral quark model.) The mass of the corresponding scalar state $I^G J^{PC} = 0^+0^{++}$ of $ss\bar{s}\bar{s}$ is calculated to be 1925 MeV, which is a little lower than the mass of scalar meson $f_0(2020)$.

By calculation the distance between quarks, we can get the spacial structure of the tetraquark. For state $Y(2175)$, the results are

$$\langle \mathbf{r}^2_{12} \rangle = \langle \mathbf{r}^2_{34} \rangle = 1.0\text{fm}^2 \tag{31}$$

$$\langle \mathbf{r}^2_{13} \rangle = \langle \mathbf{r}^2_{14} \rangle = \langle \mathbf{r}^2_{23} \rangle = \langle \mathbf{r}^2_{24} \rangle = 1.5\text{fm}^2 \tag{32}$$

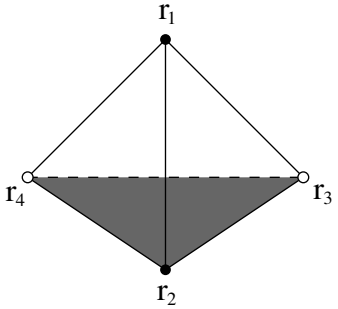

Fig. 2. Spacial structure of the $Y(2175)$

Obviously, the $Y(2175)$ can not be planar, as shown in the Fig. 2.

From Table 3, we can see an interesting phenomenon, Taking as the possible candidates of scaler meson observed experimentally, the ground states contain s, c quarks in our model have energies about 100 MeV lower than experiment values, while the excited states are consistent with experiment values. Further study is needed to clarify the situation. The reason may be that the coupling to two-quark state is missing, which the coupling will push the tetraquark state higher.

4 Unquenched Quark Model for Charmonium

To unify the description of meson, the unquenched quark model should be developed, i.e, the high Fock states, $q^2\bar{q}^2$, $q\bar{q}g$, $q^3\bar{q}^3$, gg, $\cdots$ should be coupled with $q\bar{q}$ to give the meson spectrum. As a first step, we only incorporate the four-quark components in the present work. The meson state reads

$$|\Psi\rangle = a_0|\psi_0\rangle + \sum_{BC}\int c_{BC}(\mathbf{p})|BC;\mathbf{p}\rangle d^3p, \tag{33}$$

where $|\psi_0\rangle$ represents two-quark state, and $|BC;\mathbf{p}\rangle$ represents four-quark states, which appear as two mesons with relative motion momentum $\mathbf{p}$. The meson wavefunction satisfies the following Schrödinger equation

$$H|\Psi\rangle = M|\Psi\rangle, \tag{34}$$

The system hamiltonian is

$$H = H_0 + H_{BC} + H_I. \tag{35}$$

where H_0 is the hamiltonian for two quark state, which acts on ψ_0 only,

$$H_0|\psi_0\rangle = M_0|\psi_0\rangle, \tag{36}$$

H_{BC} stands for the four-quark hamiltonian, which acts on $|BC;\mathbf{p}\rangle$ only.

$$H_{BC}|BC,\mathbf{p}\rangle = E_{BC}(\mathbf{p})|BC,\mathbf{p}\rangle, \tag{37}$$

$$E_{BC}(\mathbf{P_B},\mathbf{P_C}) = \sqrt{M_B^2+\mathbf{P}_B^2} + \sqrt{M_C^2+\mathbf{P}_C^2}, \tag{38}$$

H_I couples two-quark state $|\psi_0\rangle$ and four-quark state $|BC\rangle$. By solving the above Schrödinger equation, the mass of meson can be put as

$$M = M_0 + \Delta M, \tag{39}$$

where ΔM is the mass shift due to the channel coupling,

$$\Delta M = \sum_{BC}\int d^3p \frac{|\langle BC|H_I|\psi_0\rangle|^2}{M - E_{BC} + i\epsilon}. \tag{40}$$

For the given channel BC, the mass shift

$$\begin{aligned}\Delta M_A^{BC} &= -\int d^3p \frac{|\langle BC|H_I|\psi_0\rangle|^2}{E_{BC} - M + i\epsilon} \\ &= -\int d^3p \frac{|\mathcal{M}^{JL}|^2}{\sqrt{M_B^2+p^2}+\sqrt{M_C^2+p^2}-M},\end{aligned} \tag{41}$$

The percentage of two-quark state in the physical state of meson can also be obtained,

$$N^2 = \left[1 + \sum_{BC}\sum_{JL}\int d^3p \frac{|M^{JL}|^2}{\left(\sqrt{M_B^2+p^2}+\sqrt{M_C^2+p^2}-M\right)^2}\right]^{-1} \tag{42}$$

To calculate the transition amplitude $\mathcal{M}^{JL}$, the$^3P_0$ model, also called quark-pair creation model, which is developed to account for the strong decay of hadron [24], is used. In the model, it assumes that quark-antiquark pair are created with vacuum quantum number $J^{PC} = 0^{++}$. The diagrams of all possible decay process $A \to B + C$ of meson are shown in Fig.3. In many cases only one of them contributes to the strong decay of meson. The transition operator in the model takes the form,

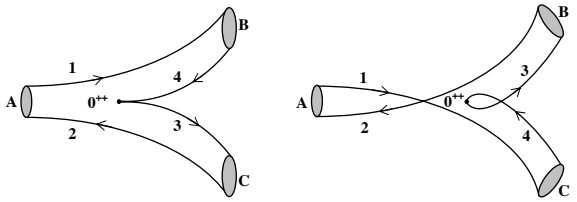

Fig.3 The two possible diagrams contributing to $A \to B + C$ in the $^3P_0$ model.

$$H_I = -3\,\gamma \sum_m \langle 1m1-m|00\rangle \int d\mathbf{p}_3 d\mathbf{p}_4 \delta^3(\mathbf{p}_3+\mathbf{p}_4)\mathcal{Y}_1^m(\frac{\mathbf{p}_3-\mathbf{p}_4}{2})\chi^{34}_{1-m}\phi_0^{34}\omega_0^{34}b_3^\dagger(\mathbf{p}_3)d_4^\dagger(\mathbf{p}_4), \tag{43}$$

where γ, which is a dimensionless parameter, represents the probability of the quark-antiquark pair created from the vacuum and can be determined by fitting the observed strong decay of hadrons. $\phi_0^{34} = (u\bar{u} + d\bar{d} + s\bar{s})/\sqrt{3}$, $\omega_0^{34} = (r\bar{r} + g\bar{g} + b\bar{b})/\sqrt{3}$ are flavor and color singlet state, respectively. $\chi^{34}_{1,-m}$ is a spin-triplet state. $\mathcal{Y}_l^m(\mathbf{p}) \equiv |p|^l Y_l^m(\theta_p, \phi_p)$ is the lth solid harmonic polynomial that reflects the momentum-space distribution of the created quark-antiquark pair. $b_3^\dagger(\mathbf{p}_3)$, $d_4^\dagger(\mathbf{p}_4)$ are the creation operators of the quark and antiquark, respectively.

In general, the mock state is adopted to describe the meson with the spatial wave function $\psi_{n_A L_A M_{L_A}}(\mathbf{p}_1, \mathbf{p}_2)$ in the momentum representation [25].

$$\begin{aligned}|A(n_A{}^{2S_A+1}L_{A\,J_A M_{J_A}})(\mathbf{P}_A)\rangle \equiv\ & \sqrt{2E_A}\sum_{M_{L_A},M_{S_A}} \langle L_A M_{L_A} S_A M_{S_A}|J_A M_{J_A}\rangle \\ & \times \int d\mathbf{p}_1 d\mathbf{p}_2 \psi_{n_A L_A M_{L_A}}(\mathbf{p}_1,\mathbf{p}_2)\chi^{12}_{S_A M_{S_A}}\phi_A^{12}\omega_A^{12}|q_1(\mathbf{p}_1)\bar{q}_2(\mathbf{p}_2)\rangle,\end{aligned} \tag{44}$$

with the normalization conditions

$$\langle A(n_A{}^{2S_A+1}L_{A\,J_A M_{J_A}})(\mathbf{P}_A)|A(n_A{}^{2S_A+1}L_{A\,J_A M_{J_A}})(\mathbf{P'}_A)\rangle = 2E_A\delta^3(\mathbf{P}_A - \mathbf{P'}_A). \tag{45}$$

where n_A represent the radial quantum number of the meson A composed of q_1, $\bar{q}_2$ with momentum $\mathbf{p_1}$ and $\mathbf{p_2}$. E_A is the total energy and $\mathbf{P}_A$ is the momentum of the meson A. $\mathbf{S}_A = \mathbf{s}_{q_1} + \mathbf{s}_{q_2}$, $\mathbf{J}_A = \mathbf{L}_A + \mathbf{S}_A$ stand for the total spin and total angular momentum, respectively. $\mathbf{L}_A$ is the relative orbital angular momentum between q_1 and $\bar{q}_2$. $\langle L_A M_{L_A} S_A M_{S_A}|J_A M_{J_A}\rangle$ denotes a Clebsch-Gordan coefficient, and $\chi^{12}_{S_A M_{S_A}}$, ϕ_A^{12} and ω_A^{12} are the spin, flavor and color wave functions, respectively.

By using the above transition operator and the meson wave functions, The transition matrix element can be calculated,

$$\langle BC|H_I|A\rangle = \delta^3(\mathbf{P}_A - \mathbf{P}_B - \mathbf{P}_C)\mathcal{M}^{M_{J_A}M_{J_B}M_{J_C}}, \tag{46}$$

where $\mathcal{M}^{M_{J_A}M_{J_B}M_{J_C}}$ is the helicity amplitude of $A \to B + C$. In the center of mass frame of meson A, $\mathbf{P}_A = 0$, and $\mathcal{M}^{M_{J_A}M_{J_B}M_{J_C}}$ can be written as (color factor gives 1/3)

$$\begin{aligned}\mathcal{M}^{M_{J_A}M_{J_B}M_{J_C}}(\mathbf{P}) = \gamma\sqrt{8E_AE_BE_C}\sum_{\text{all } m\text{'s}} & \langle L_A M_{L_A} S_A M_{S_A}|J_A M_{J_A}\rangle\langle L_B M_{L_B} S_B M_{S_B}|J_B M_{J_B}\rangle \\ \times \langle L_C M_{L_C} S_C M_{S_C}|J_C M_{J_C}\rangle & \langle 1m1-m|00\rangle\langle\chi^{14}_{S_B M_{S_B}}\chi^{32}_{S_C M_{S_C}}|\chi^{12}_{S_A M_{S_A}}\chi^{34}_{1-m}\rangle\Big[\langle\phi_B^{14}\phi_C^{32}|\phi_A^{12}\phi_0^{34}\rangle \\ \times \mathcal{I}^{M_{L_A},m}_{M_{L_B},M_{L_C}}(\mathbf{P},m_1,m_2,m_3) + (-1)^{1+S_A+S_B+S_C}&\langle\phi_B^{32}\phi_C^{14}|\phi_A^{12}\phi_0^{34}\rangle\mathcal{I}^{M_{L_A},m}_{M_{L_B},M_{L_C}}(-\mathbf{P},m_2,m_1,m_3)\Big],\end{aligned} \tag{47}$$

with the momentum space integral,

$$\mathcal{I}^{M_{L_A},m}_{M_{L_B},M_{L_C}} = \int d\mathbf{p}\,\psi^*_{n_B L_B M_{L_B}}(\tfrac{m_3}{m_1+m_3}\mathbf{P}+\mathbf{p})\psi^*_{n_C L_C M_{L_C}}(\tfrac{m_3}{m_2+m_3}\mathbf{P}+\mathbf{p})\psi_{n_A L_A M_{L_A}}(\mathbf{P}+\mathbf{p})\mathcal{Y}^m_1(\mathbf{p}), \tag{48}$$

where $\mathbf{P}=\mathbf{P}_B=-\mathbf{P}_C$, $\mathbf{p}=\mathbf{p}_3$, m_3 is the mass of the created quark q_3; $\langle\chi^{14}_{S_B M_{S_B}}\chi^{32}_{S_C M_{S_C}}|\chi^{12}_{S_A M_{S_A}}\chi^{34}_{1-m}\rangle$ and $\langle\phi^{14}_B\phi^{32}_C|\phi^{12}_A\phi^{34}_0\rangle$ are the overlap of spin and flavor wave functions, respectively.

The flavor overlap can be evaluated directly and the spin overlap can be obtained in terms of Winger's $9j$ symbol,

$$\langle\chi^{14}_{S_B M_{S_B}}\chi^{32}_{S_C M_{S_C}}|\chi^{12}_{S_A M_{S_A}}\chi^{34}_{1-m}\rangle = \sum_{S,M_S}\langle S_B M_{S_B} S_C M_{S_C}|S\,M_S\rangle\langle S_A M_{S_A}\,1-m|S\,M_S\rangle$$
$$\times(-1)^{S_C+1}\sqrt{3(2S_A+1)(2S_B+1)(2S_C+1)}\begin{Bmatrix}\frac{1}{2} & \frac{1}{2} & S_A\\ \frac{1}{2} & \frac{1}{2} & 1\\ S_B & S_C & S\end{Bmatrix}. \tag{49}$$

To evaluate the momentum space integral, the space wave function must be fixed. Generally, one takes the simple harmonic oscillator (SHO) approximation for the meson space wave functions. It reads

$$\Psi_{nLM_L}(\mathbf{p}) = (-1)^n(-i)^L R^{L+\frac{3}{2}}\sqrt{\frac{2n!}{\Gamma(n+L+\frac{3}{2})}}\exp\left(-\frac{R^2p^2}{2}\right)L_n^{L+\frac{1}{2}}\left(R^2p^2\right)\mathcal{Y}_{LM_L}(\mathbf{p}), \tag{50}$$

with $\mathcal{Y}_{LM_L}(\mathbf{p}) = |\mathbf{p}|^L Y_{LM_L}(\Omega_p)$. Here R denotes the SHO wave function scale parameter, which is fixed by fitting the wave function obtained by solving Schödinger equation of the corresponding meson; $\mathbf{p}$ represents the relative momentum between the quark and the antiquark within a meson; $L_n^{L+\frac{1}{2}}\left(R^2p^2\right)$ is an associated Laguerre polynomial.

The partial-wave amplitude in Eq.(41) can be related to the helicity amplitude in Eq.(47) via the Jacob-Wick formula [26]

$$\mathcal{M}^{JL}(A\to BC) = \frac{\sqrt{2L+1}}{2J_A+1}\sum_{M_{J_B},M_{J_C}}\langle L0JM_{J_A}|J_AM_{J_A}\rangle\langle J_BM_{J_B}J_CM_{J_C}|JM_{J_A}\rangle\mathcal{M}^{M_{J_A}M_{J_B}M_{J_C}}(\mathbf{P}), \tag{51}$$

where $\mathbf{J}=\mathbf{J}_B+\mathbf{J}_C$, $\mathbf{J}_A=\mathbf{J}_B+\mathbf{J}_C+\mathbf{L}$,and $M_{J_A}=M_{J_B}+M_{J_C}$.

Combining Eqs.(41), (49) and (51), the mass shift can be obtained. To be noted that the physical mass M also appears at the right-hand side of Eq.(41), the iteration method should be used here. First by setting $M=M_A$, the mass shift ΔM and the new physical mass are obtained, then substituting new physical mass in the Eq.(41), the new mass shift is obtained. Continue this process until a stable physical mass is reached.

Recently the mass shifts for charmonium, bottomonium and other mesons have been calculated by several groups [27]. The results show that the mass shifts are rather large, especially for the light mesons. So the contribution from the four-quark components cannot be ignored. Of course, part of the effects can be absorbed by the model parameters. It is very interesting to see that can the unquenched quark model improve the agreement between theoretical results and the experimental data? In the following, we take charmonium as an example, adjusting the model parameters and re-fitting the experimental data by incorporating the four-quark components in the quark model.

Table 4. The re-adjusted parameters.

$m_u=m_d$ (MeV)	m_s (MeV)	m_c (MeV)	$\alpha_s(c\bar{c})$	$\alpha_s(c\bar{q})$
321	587	1758	0.40	0.58

The model parameters of the unquenched quark model for charmonium is listed in Table 4. As a preliminary study, only the masses of quarks and the coupling constant α_s of OGE are re-adjusted, other parameters keep their value in the model without high Fock components. $\gamma=6.95$ and $\gamma_s=\gamma/\sqrt{3}$ [28]. The calculated charmonium spectrum is shown in Table 5.

Table 5. The masses of charmonium $c\bar{c}$ (unit: MeV).

$n^{2S+1}L_J$	β (GeV)	$c\bar{c}$ mass	mass shift	physical mass	exp. mass	$c\bar{c}$ ratio (%)
1^1S_0	0.730	3163	-184	2979	2980.3±1.2	92.75
2^1S_0	0.560	3850	-216	3634	3637±4	88.90
3^1S_0	0.478	4250	-190	4060		87.99
4^1S_0	0.390-0.446	4527	-140 -165	4387-4362		89.62-87.74
5^1S_0	0.360-0.390	4727	-123 -131	4604-4596		-
1^3S_1	0.632	3295	-186	3109	3096.916±0.011	91.80
2^3S_1	0.504	3918	-208	3710	3686.09±0.04	88.16
3^3S_1	0.446	4296	-181	4115		87.62
4^3S_1	0.366-0.424	4560	-135 -159	4425-4401		-
5^3S_1	0.348-0.374	4751	-121 -128	4630-4623		-
1^1P_1	0.528	3723	-207	3516	3525.93±0.27	88.93
2^1P_1	0.462	4157	-194	3963		87.30
3^1P_1	0.398	4457	-151	4306		88.27
4^1P_1	0.366-0.398	4674	-129 -140	4545-4534		-
5^1P_1	0.332-0.366	4833	-112 -118	4721-4715		-
1^3P_0	0.526	3662	-199	3463	3414.75±0.31	89.58
2^3P_0	0.460	4114	-187	3927		87.93
3^3P_0	0.396	4425	-147	4278		88.81
4^3P_0	0.366-0.398	4654	-126 -138	4528-4517		-
5^3P_0	0.332-0.366	4815	-111 -116	4704-4699		-
1^3P_1	0.526	3693	-202	3491	3510.66±0.07	89.31
2^3P_1	0.460	4137	-190	3947		87.67
3^3P_1	0.396	4442	-148	4294		88.65
4^3P_1	0.366-0.39	4665	-127 -136	4538-4529		-
5^3P_1	0.332-0.366	4824	-111 -117	4713-4707		-
1^3P_2	0.526	3757	-213	3544	3556.93±0.27	88.42
2^3P_2	0.460	4181	-197	3984		86.83
3^3P_2	0.396	4476	-154	4322		87.77
4^3P_2	0.366-0.39	4687	-131 -143	4556-4544		-
5^3P_2	0.332-0.366	4844	-114 -120	4730-4724		-
1^1D_2	0.462	4027	-200	3827		86.91
2^1D_2	0.418	4361	-167	4194		86.94
3^1D_2	0.376	4603	-134	4469		87.57
4^1D_2	0.336-0.376	4781	-113 -121	4668-4660		-
5^1D_2	0.296-0.336	4910	-102 -105	4808-4805		-
1^3D_1	0.462	4003	-197	3806		87.23
2^3D_1	0.418	4343	-165	4178		87.16
3^3D_1	0.376	4590	-132	4458		-
4^3D_1	0.336-0.376	4770	-111 -121	4659-4649		-
5^3D_1	0.296-0.336	4902	-102 -104	4800-4798		-
1^3D_2	0.462	4019	-199	3820		87.06
2^3D_2	0.418	4355	-166	4189		87.06
3^3D_2	0.376	4599	-134	4465		87.59
4^3D_2	0.336-0.376	4777	-112 -121	4665-4656		-
5^3D_2	0.296-0.336	4907	-101 -104	4806-4803		-
1^3D_3	0.462	4043	-204	3839		86.56
2^3D_3	0.418	4373	-170	4203		86.63
3^3D_3	0.376	4614	-137	4477		-
4^3D_3	0.336-0.376	4788	-114 -123	4674-4665		-
5^3D_3	0.296-0.336	4915	-103 -106	4812-4809		-

There are several features of our calculation:

(1) From Table 5, we can see the percentages of $c\bar{c}$ in the physical states are all around 90%, which are different from the results of the previous work (where the percentage may be as low as 50% in P-wave states). The high percentage of $c\bar{c}$ is a welcome property, which make our calculation consistent, the higher Fock states, $q^3\bar{q}^3$, $\cdots$ can be neglected safely.

(2) The mass shifts for the states with the same n, L are almost same, which is consistent with other calculation [27,29].

(3) The experimental masses below the $D\bar{D}$ threshold are reproduced well, similar to the results of the quenched quark model (only $c\bar{c}$ component). This means that for the low-lying states, the four-quark contributions can be totally absorbed into the parameters. For the states $\psi(3770)$, $\psi(4040)$, $\psi(4160)$ and $\psi(4415)$, the model gives the masses close to experimental data, if these states are taken as 1^3D_1, 3^3S_1 , 2^3D_1 and 4^3S_1.

(4) For given J, L, The mass shifts for small n is larger than that for large n. This feature leads to that the high states will be pushed higher, which it cannot be absorbed into parameters of the quenched quark model.

(5) As for the new charmonia (XYZ particles) observed in recent years [2], some states can be identified as states in Table 5, some states cannot be allocated due to their possible exotic structures, tetraquark, glueball, molecule, hybrid, etc. [2]. The assignments are listed in Table 6. To keep in mind, these assignments are based on the masses only. To validate the assignments, decay properties calculation of these states needs to be done.

Table 6. The assignments of XYZ states.

states	$X(3872)$	$X(3915)$	$Z(3930)$	$X(3940)$	$Y(3940)$
assignment	1^1D_2	2^3P_0	2^3P_2	2^3P_1	2^1P_1
mass (MeV)	3827	3927	3984	3947	3963
states	$X(4140)$	$X(4160)$	$X(4350)$	$Y(4630)$	$Y(4660)$
assignment	2^1D_2	2^1D_2	3^3P_2	5^3S_1	4^3D_1
mass (MeV)	4194	4194	4322	4630	4659

5 Summary

The non-relativistic quark model has achieved great success in describing the properties of hadrons, especially for the low-lying states. With advance of experiments, more excited states are observed, the quark model should be developed. Unquenching thequark model is an important step for the development. How to unquench the quark model is still an open question. In the present work, the commonly used $^3P_0$ model is employed and the unquenched quark model is applied to explore the charmonium spectrum. The calculation shows that the effects of including the four-quark component will affect the masses of highly excited states while keeping the agreement between theoretical results and experimental data for the low-lying states. The calculation also shows that the higher Fock states, $q^3\bar{q}^3$ can be neglected safely. The further work on unquenching quark model is to improve the wave functions of created quark-pair, the approximation of plane wave is used at the moment.

Another development of quark model is to study the multi-quark system, where the multi-body interaction may play an important role. Based on the lattice QCD calculation, a string (flux-tube) model is proposed to study the tetraquark system. The calculated results are encouraging, most of the scalar mesons can be described as tetraquark states in the model. An important feature of the model is that an alternative form of color confinement is used. So the multi-quark system is a good place to check the validity of the Casimir scaling [16].

Another problem to be solved is how to coupling the Fock states with different color structures. String model is a good starting point. The mechanism to break and re-join the string needs to clarify.

Acknowledgment

This work is supported partly by the National Science Foundation of China under Contract Nos. 11035006, 10775072, 11047140 and 10947160, the Research Fund for the Doctoral Program of Higher

Education of China under Grant No. 20070319007 and the PhD Program Funds of Chongqing Jiaotong University.

References

1. C. R. Deng, J. L. Ping, F. Wang and T. Goldman, Phys. Rev. D82 (2010) 074001.
2. N. Brambilla, S. Eidelman, B. K. Heltsley, *et al*, Eur. Phys. J. C71 (2011) 1534 and references therein.
3. A. Manohar and H. Georgi, Nucl. Phys. B234 (1984) 189.
4. J. Vijande, F. Fernandez and A. Valcarce, J. Phys. G31 (2005) 481.
5. L. Z. Chen, H. R. Pang, H. X. Huang, J. L. Ping and F. Wang, Phys. Rev. C76 (2007) 014001.
6. R. K. Bhaduri, L. E. Cohler and Y. Nogami, Phys. Rev. Lett. 44 (1980) 1369.
7. J. Weinstein and N. Isgur, Phys. Rev. D27 (1983) 588.
8. E. Hiyama, Y. Kino and M. Kamimura, Prog. Part. Nucl. Phys. 51 (2003) 223.
9. L. Wang, J. L. Ping, Chin. Phys. Lett. 24 (2007) 1195.
10. T. T. Takahashi, H. Matsufuru, Y. Nemoto and H. Suganuma, Phys. Rev. Lett. 86 (2001) 18; T. T. Takahashi, H. Suganuma, Y. Nemoto and H. Matsufuru, Phys. Rev. D65 (2002) 114509; F. Okiharu, H. Suganuma and T. T. Takahashi, Phys. Rev. Lett. 94 (2005) 192001.
11. L. Maiani, F. Piccinini, A. D. Polosa *et al*, Phys. Rev. Lett. 93 (2004) 21.
12. L. Maiani, V. Riquer, F. Piccinini and A.D. Polosa, Phys. Rev. D72 (2005) 031502.
13. M. Iwasaki and T. Fukutome Phys. Rev. D72 (2005) 094016.
14. G. J. Ding and M. L. Yan, Phys. Lett. B643 (2006) 33.
15. K. Johnson and C.B. Thorn, Phys. Rev. D13 (1976) 1934; C. Semay, Eur. Phys. J. A22 (2004) 353.
16. G. S. Bali, Phys. Rev. D62 (2000) 114503.
17. H. X. Chen, A. Hosaka and S. L. Zhu, Phys. Rev. D76 (2007) 094025.
18. B. Aubert *et al* [BABAR Collaboration], Phys. Rev. D74 (2006) 091103; Phys. Rev. D76 (2007) 012008; D77 (2008) 092002.
19. M. Ablikim *et al* [BES Collaboration], Phys. Rev. Lett. 100 (2008) 102003.
20. G. J. Ding and M. L. Yan, Phys. Lett. B650 (2007) 390; B657 (2007) 49.
21. Z. G. Wang, Nucl. Phys. A791 (2007) 106.
22. S. L. Zhu, Int. J. Mod. Phys. E17 (2008) 283.
23. A. M. Torres, K. P. Khemchandani, L. S. Geng *et al*, Phys. Rev. D78 (2008) 074031.
24. L. Micu, Nucl. Phys. B10 (1969) 521; A.Le Yaouanc, L. Oliver, O. Pene and J-C. Raynal, Phys. Rev. D8 (1973) 2223; 9(1974) 1415; 11 (1975) 1272; W. Roberts and B. Silvestr-Brac, Few-Body Syst. 11 (1992) 171; E. S. Ackleh, T. Barnes and E. S. Swanson, Phys. Rev. D54 (1996) 6811; T. Barnes, S. Godfrey and E. S. Swanson, Phys. Rev. D72 (2005) 054026.
25. C. Hayne and N. Isgur, Phys. Rev. D25 (1982) 1944.
26. M. Jacob and G. C. Wick, Ann. Phys. (Leipzig) 7 (1959) 404; Ann. Phys. (N.Y.) 281 (2000) 774.
27. T. Barnes and E. S. Swanson, Phys. Rev. C77 (2008) 055206; Yu. S. Kalashinikova, Phys. Rev. D72 (2005) 034010; B. Q. Li, C. Meng and K. T. Chao, Phys. Rev. D80 (2009) 014012.
28. H. G. Blundell and S. Godfrey, Phys. Rev. D53 (1996) 3700; D53 (1996) 3712; J. Lu, W. Z. Deng, X. L. Chen and S. L. Zhu, Phys. Rev. D73 (2006) 054012.
29. F. E. Close and C. E. Thomas, Phys. Rev. C79 (2009) 045201.